Synthesis and characterisation of lead metallated non-peripherally substituted octa-octyl tetrabenzo(aza)porphyrins showing face-to-face columnar stacking in the crystal phase

Lydia Sosa-Vargas,[a, b] Simon J Coles,[c] Graham J Tizzard,[c] Isabelle Chambrier,[a] Michael J Cook,[a]* Andrew N Cammidge,[a]*

[a] *School of Chemistry, University of East Anglia, Norwich Research Park, Norwich NR4 7TJ, UK*

[b] *Current address : Sorbonne Université, CNRS, Institut Parisien de Chimie Moléculaire (IPCM), Paris, France*

[c] *EPSRC National Crystallography Service, School of Chemistry, University of Southampton, Southampton SO17 1BJ, IK*

Received date (to be automatically inserted after your manuscript is submitted)
Accepted date (to be automatically inserted after your manuscript is accepted)

ABSTRACT: The full range of porphyrin-phthalocyanine hybrids can be synthesised by treatment of 1,4-dioctylphthalonitrile with varying equivalents of MeMgBr to produce mixtures favouring specific hybrid structures and the tetrabenzoporphyrin in the extreme case. The individual macrocycles can be isolated in pure form as their magnesium derivatives, and subsequently demetallated to give the parent metal-free compounds. Insertion of lead proceeded smoothly with all hybrids using lead (II) acetate. In the case of monoaza- and triaza-hybrids, the resulting materials could be recrystallised to give crystals suitable for X-ray diffraction. The crystal structures are distinctive from previously reported examples of non-peripherally substituted octaalkyl phthalocyanines and hybrids (metal-free and metallated, including with lead) and they each present infinite stacks of cofacial macrocycles linked through bridging lead ions which, as expected, lie outside of the macrocycle plane.

KEYWORDS: Lead Phthalocyanines, Phthalocyanine-Porphyrin hybrids, Crystal Structure, Columnar Stacks.

*Correspondence to: Andrew N Cammidge, email: a.cammidge@uea.ac.uk, tel: +44 (0)1603-592011.

INTRODUCTION

Tetrabenzo(aza)porphyrin hybrids are intermediate structures that lie between phthalocyanines and (tetrabenzo)porphyrins, and they can be defined as the structures depicted when 1, 2 (two isomers) or 3 of the bridging ("meso") nitrogens of a phthalocyanine are replaced by carbon bridges (Figure 1). Early syntheses of hybrid compounds undertaken independently by Heilberger, Dent and Linstead [1] in the 1930s utilised reactions of phthalonitrile with methyl magnesium iodide, methyllithium or phthalimidine acetic acid. The groups of Galanin [2], Leznoff [3], Luk'yanets [4], and others [5], extended both the chemistry and the range of derivatives available, leading to the synthesis of examples of all four hybrid

compounds. Particular attention has been given to the incorporation of substituents on the benzenoid rings and/or at the *meso* carbon atoms and the area has been reviewed [6]. In addition, our group and others have developed and studied new synthetic routes, significantly overcoming some of the initial issues [7-10]. Most recently we have disclosed additional control in the synthesis of TBTAPs that permits direct access to *meso*-aryl 3:1 (ABBB-Ar) and 2:2 (ABBA-Ar) derivatives [11] (Figure 1, inset).

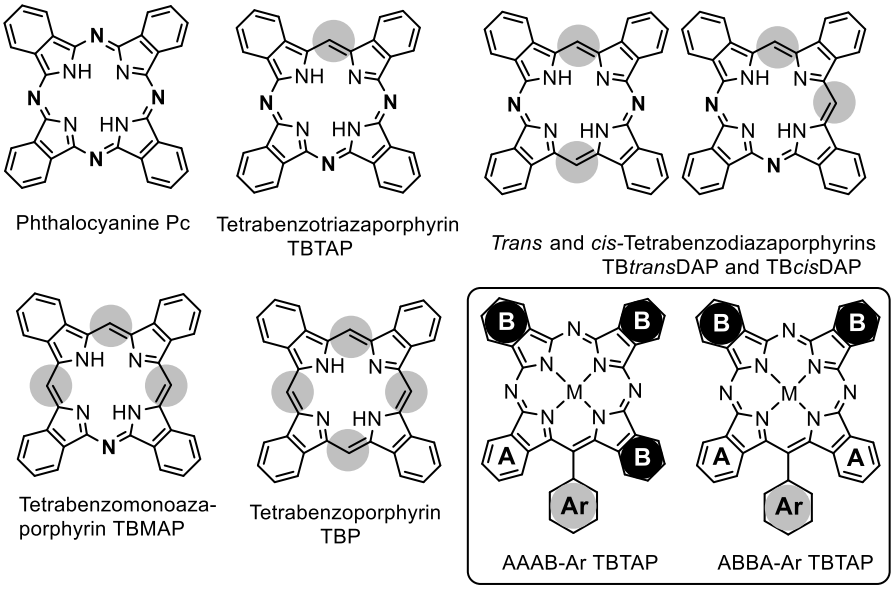

Figure 1. The parent structures of the phthalocyanine-tetrabenzoporphyrin hybrids and a recent example of structural variation across benzo- and *meso* positions in tetrabenzotriazaporphyrins (TBTAPS) (inset [11]).

In some of our earliest work on hybrids we discovered that introduction of (alkyl) substituents at the non-peripheral benzo positions prevented incorporation of any bulky functionality at the neighboring *meso* site [5c]. Indeed, when reactions with 1,4-dialkyl phthalonitriles were initiated with Grignard or lithium reagents other than methyl (i.e. other than MeMgX or MeLi), the resulting TBTAP hybrid that was isolated always only included a hydrogen bonded at the *meso* position, with the rest of the initiator chain lost at some stage of the reaction [5c]. Consequently, in all subsequent reaction development, we employed only MeMgBr, finding that careful reaction control could favor formation of specific hybrids. When a large excess of Grignard reagent is used the major isolated macrocycle is in fact the tetrabenzoporphyrin [8] (Scheme 1).

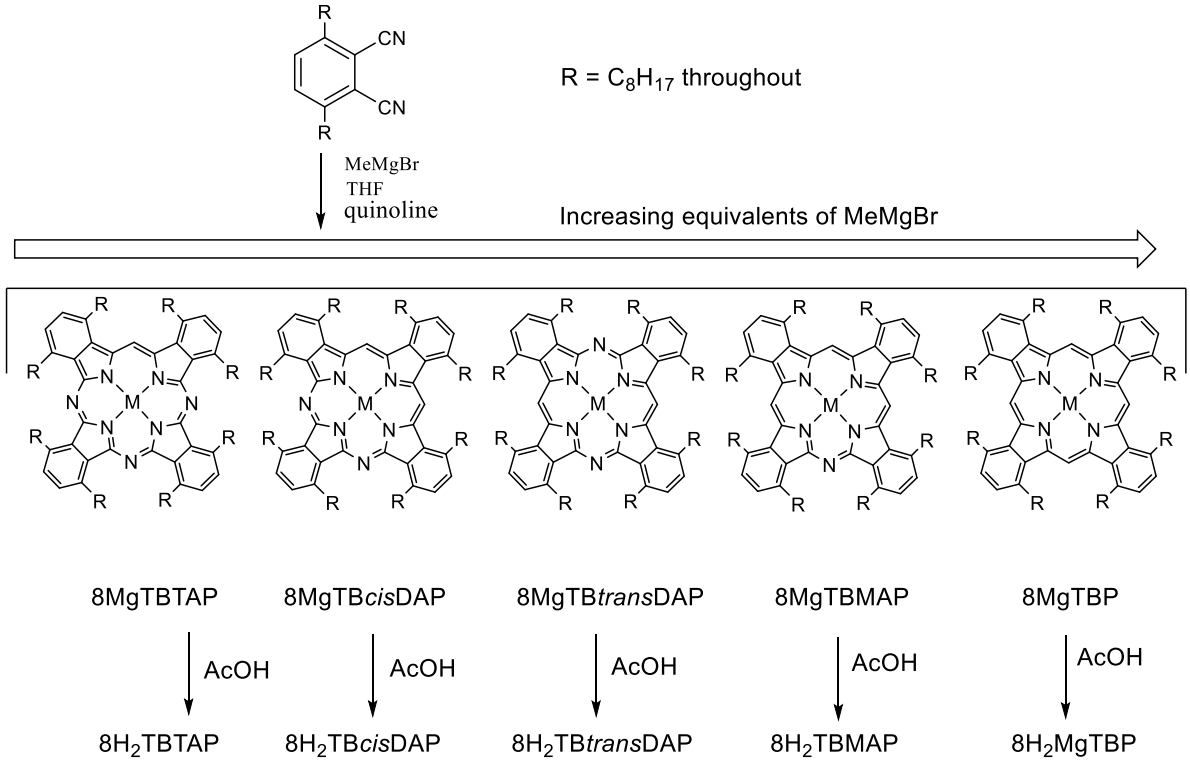

Scheme 1. Synthesis of the full range of magnesium and metal-free hybrid macrocycles bearing n-octyl chains ("8") on the non-peripheral benzo-sites [8b].

EXPERIMENTAL

General methods

^{1}H NMR spectra at 400 MHz were recorded on an Ultrashield Plus^{TM} 400 spectrometer and at 500 MHz on a Bruker Ascend 500 instrument. Signals are quoted in ppm as δ downfield from tetramethylsilane (δ= 0.00) with residual solvent peaks used as reference. ^{13}C NMR spectra could not be obtained due to aggregation and precipitation at higher concentrations. Ultra-violet spectra were recorded using a PerkinElmer Lambda 365 spectrophotometer. Mass analysis was undertaken using a Shimadzu MALDI-TOF spectrometer with a TA1586Ade plate and DCTB as matrix and calibrated against 1,4,8,11,15,18,22,25-octaoctyl phthalocyanine. Isotopic distribution patterns matched calculated relative intensity profiles. Column chromatography was performed at ambient temperature using Aldrich® neutral alumina with solvent systems given as volume ratios.

X-Ray diffraction was performed at the EPSRC Service Centre (University of Southampton) on a Rigaku FRE+ diffractometer equipped with VHF Varimax confocal mirrors and an AFC12 goniometer and HG Saturn 724+ detector. The crystal was kept at a steady T = 100(2) K during data collection. The structure was solved with the ShelXT 2018/2 [12] structure solution program using the dual methods solution method and by using Olex2 1.5-alpha [13] as the graphical interface. The model was refined with olex2.refine 1.5-alpha [14] using full matrix least squares minimisation on $\boldsymbol{F}^2$ minimisation.

Magnesium and metal-free octaoctyl hybrid macrocycles and tetrabenzoporphyrins were synthesised as previously reported [8].

Synthesis of lead tetrabenzo(aza)porphyrin derivatives – typical procedure for ***1,4,8,11,15,18,22,25-octakis(octyl)-tetrabenzo[b,g,l,q]-[5,10,15]triaza porphinato lead 8PbTBTAP***

1,4,8,11,15,18,22,25-Octakis(octyl)-tetrabenzo[*b,g,l,q*][5,10,15]triazaporphyrin **8H$_2$TBTAP** (20.0 mg, 0.014 mmol) was dispersed together with lead acetate trihydrate (8.1 mg, 0.022 mmol) in pentanol (10.0 mL) using an ultrasonic bath. The dispersed mixture was stirred and heated to reflux for 15 minutes. After cooling, the product was precipitated by addition of distilled water, extracted with DCM and washed repeatedly with water to remove inorganic residues. The organic extract was dried with Na_2SO_4 and the solvent evaporated to give the expected product as a light-green fine powder. Purification by column chromatography using neutral alumina as the stationary phase and DCM as eluent gave the product as a single fraction which, after re-crystallisation using DCM/MeOH, yielded **8PbTBTAP** as fine, green crystals (16.0 mg, 70%). MALDI-MS: isotopic cluster at m/z 1615 [100%, M^+], ^{1}H NMR (500 MHz, toluene-d$_8$, ppm) 11.07 (1H, s), 7.97-7.94 (6H, m), 7.85 (2H, br-d, J = 7.0 Hz), 5.08-4.93 (6H, br-m), 4.92-4.67 (6H, br-m), 4.41-4.29 (2H, br-m), 4.13-4.04 (2H, br-m), 2.49-2.35 (16H, m), 1.86-1.68 (16H, br-m), 1.46-1.13 (64H, m), 0.94-0.79 (24H, m), λ_{max} (log ε) (dichloromethane) 744 (5.13), 710 (5.13), 677 (4.99), 498 (4.85) nm.

Crystal Data. $C_{97}H_{145}N_7Pb$, M_r = 1616.497, tetragonal, *P*4*cc* (No. 103), a = 23.4355(4) Å, b = 23.4355(4) Å, c = 7.8133(4) Å, $a = b = g = 90^\circ$, V = 4291.2(2) Å^3, T = 100(2) K, Z = 2, Z' = 0.25, m(Mo K$_a$) = 2.016 mm^{-1}, 23363 reflections measured, 4512 unique (R_{int} = 0.0931) which were used in all calculations. The final wR_2 was 0.1412 (all data) and R_1 was 0.0520 (I≥2 *s*(I)). Further crystal structure detail is given in the Supporting Information.

1,4,8,11,15,18,22,25-Octakis(octyl)-tetrabenzo[b,g,l,q][5,10] diazaporphinato lead 8PbTBcisDAP

Prepared as above from **8H$_2$TB*cis*DAP** (10.0 mg, 0.007 mmol) and lead acetate trihydrate (4.0 mg, 0.011 mmol) to give **8PbTB*cis*DAP** as a green solid (7.8 mg, 68%). MALDI-MS: isotopic cluster at m/z 1614 [100%, M^+]. ^{1}H NMR (400 MHz, toluene-d$_8$, ppm) 11.17 (2H, s), 7.98 (2H, s), 7.96 (2H, d J = 8.0 Hz), 7.87 (2H, d, J = 8.0 Hz), 7.82 (2H, s), 5.15 (2H, dt, J = 14.0, 7.0 Hz), 5.00 (4H, t, J = 7.0 Hz), 4.75 (2H, dt, J = 15.0, 6.0 Hz), 4.48-4.37 (4H, m), 4.25-4.07 (4H, m), 2.55-2.10 (16H, m), 2.05-2.00 (16H, m), 1.50-1.20 (64H, m), 0.91-0.80 (24H, m). λ_{max} (dichloromethane) 698, 483 nm.

1,4,8,11,15,18,22,25-Octakis(octyl)-tetrabenzo[b,g,l,q][5,15] diazaporphinato lead 8PbTBtransDAP

Prepared as above from **8H$_2$TB*trans*DAP** (10.0 mg, 0.007 mmol) and lead acetate trihydrate (4.0 mg, 0.011 mmol) to give **8PbTB*trans*DAP** as a green solid (8.1 mg, 70%). MALDI-MS: isotopic cluster at m/z 1614 [100%, M^+]. ^{1}H NMR (500 MHz, CD_2Cl_2, ppm) 11.20 (2H, s), 7.96 (8H, s), 4.80 (4H, dt, J = 14.0, 8.0 Hz), 4.68 (4H, dt, J = 14.0, 7.5 Hz), 4.46 (4H, dt, J = 15.0, 7.0 Hz), 4.25 (4H, dt, J = 16.0, 8.0 Hz), 2.48-239 (8H, m), 2.22-2.11 (8H, m) 1.82-1.68 (8H, m), 1.63-1.54 (8H, m) 1.52-1.12 (64H, m), 0.87-0.82 (12H, m), 0.79-0.74 (12H, m). λ_{max} (dichloromethane) 737, 702, 655, 499 nm.

1,4,8,11,15,18,22,25-Octakis(octyl)-tetrabenzo[b,g,l,q][5] monoazaporphinato lead 8PbTBMAP

Prepared as above from **8H$_2$TBMAP** (20.0 mg, 0.014 mmol) and lead acetate trihydrate (8.1 mg, 0.022 mmol) to give **8PbTBMAP** as small black needle-like crystals (17.2 mg, 75%). MALDI-MS: isotopic cluster at m/z 1613 [100%, M^+]. ^{1}H NMR (500 MHz, toluene-d$_8$, ppm) 11.51 (1H, s), 11.36 (2H, s), 8.05 (2H, d, J = 8.0 Hz), 7.96 (2H, d, J = 8.0 Hz), 7.92 (4H, s), 5.22 (2H, dt, J = 14.0, 8.0 Hz), 5.08 (2H, dt, J = 14.0, 8.0 Hz), 4.63-4.53 (8H, m), 4.42-4.23 (4H, m), 2.60-2.43 (16H, m), 1.88-1.77 (16H, m), 1.55-1.15 (64H, m), 0.95-0.77 (24H, m). λ_{max} (log ε) (dichloromethane) 699 (5.46), 680 (5.24), 654 (5.15), 499 (5.43) nm.

Crystal Data. $C_{99}H_{147}N_5Pb$, M_r = 1614.521, tetragonal, *P*4*cc* (No. 103), a = 23.5055(4) Å, b = 23.5055(4) Å, c = 7.7588(4) Å, $a = b = g = 90^{\circ}$, V = 4286.8(2) Å^3, T = 100(2) K, Z = 2, Z' = 0.25, m(Mo K_a) = 2.017 mm^{-1}, 24700 reflections measured, 4898 unique (R_{int} = 0.0766) which were used in all calculations. The final wR_2 was 0.1091 (all data) and R_1 was 0.0430 (I≥2 *s*(I)). Further crystal structure detail is given in the Supporting Information.

1,4,8,11,15,18,22,25-Octakis(octyl)-tetrabenzo[b,g,l,q]porphinato lead 8PbTBP

Prepared as above from **8H$_2$TBP** (10.0 mg, 0.007 mmol) and lead acetate trihydrate (4.0 mg, 0.011 mmol) to give **8PbTBP** as a black-brown solid (6.9 mg, 60%). MALDI-MS: isotopic cluster at m/z 1612 [100%, M^+]. ^{1}H NMR (500 MHz, CD_2Cl_2, ppm) 11.38 (4H, br-s), 8.02 (8H, s), 4.60-4.48 (8H, br-m), 4.44-4.32 (8H, br-m), 2.54-2.39 (16H, m), 1.83-1.70 (16H, m), 1.55-1.219 (64H, m), 0.92-0.78 (24H, m). λ_{max} (dichloromethane) 677, 632, 500 nm.

RESULTS AND DISCUSSION

The full range of magnesium hybrids were prepared by treating 1,4-dioctylphthalonitrile with MeMgBr (varying equivalents) followed by heating in quinoline. The individual compounds were isolated in pure form by chromatography and subsequently demetallated using acetic acid, as described earlier [8]. Each hybrid (and the tetrabenzoporphyrin) was treated with lead acetate in refluxing pentanol - conditions developed for introduction of lead into the parent phthalocyanines [15]. Pure materials were obtained by chromatography on neutral alumina followed by recrystallization.

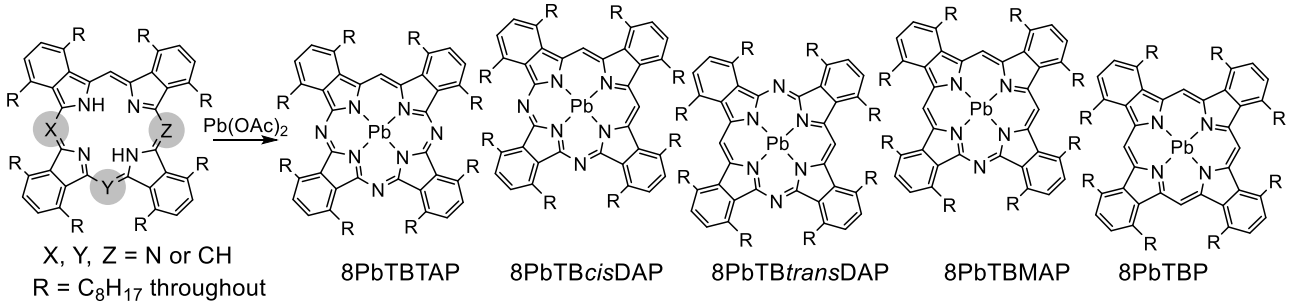

Scheme 2. Synthesis of the lead hybrid macrocycles.

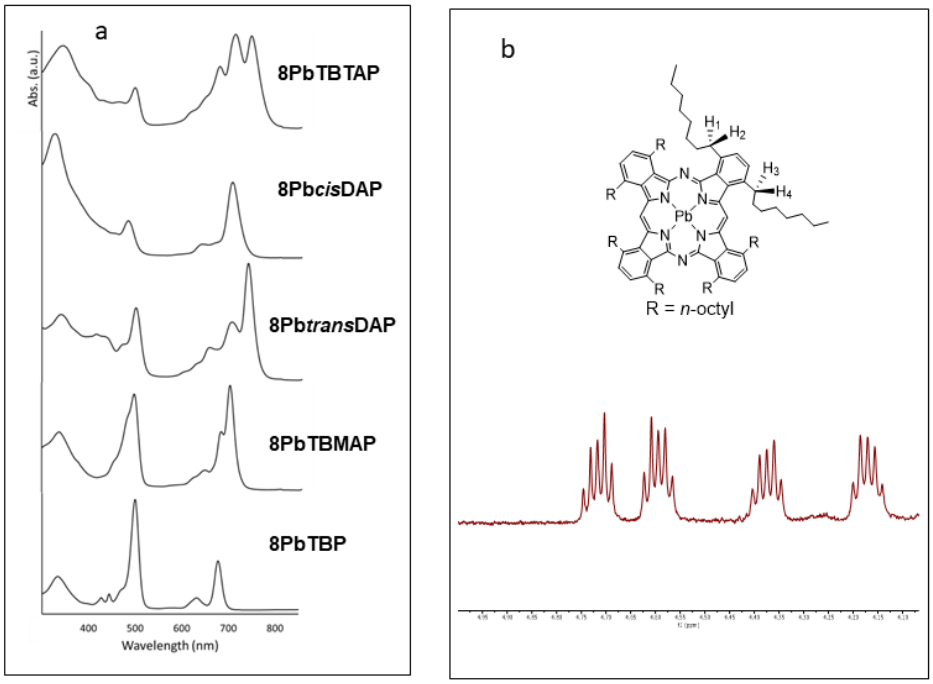

Figure 2. a) UV-visible spectra of the series of hybrids in dichloromethane. b) Expansion of the 4-5 ppm (benzylic proton) region of the ^{1}H NMR spectrum of **8Pb*trans*DAP** (in CD_2Cl_2).

UV-visible spectra for the series of lead hybrids are shown in Figure 2. They follow the general trends observed for other metalated hybrids but are each red-shifted by 40-50 nm compared to the magnesium and copper derivatives [8]. As expected, the spectra for mono- and triaza derivatives show significant reduction of symmetry in the core, and the porphyrin-like Soret band at ca 500 nm increases in relative intensity as the core nitrogens are replaced by methines. The loss of symmetry is also clearly observed in the ^{1}H NMR spectra through the series. The spectra also demonstrate that the Pb lies out of the macrocycle plane in each system, resulting in the benzylic protons becoming diastereotopic. This is most clearly seen for the higher symmetry **8Pb*trans*DAP** derivative, and the relevant region of the expanded spectrum is shown in Figure 2b. The 1H NMR spectra for all derivatives are shown in the Supporting Information.

The lead monoaza- and triaza-hybrids **8PbTBTAP** and **8PbTBMAP** were obtained as crystalline samples in sufficient quantity to allow more detailed assessment of their properties. The non-peripherally octalkyl substituted phthalocyanines are well known to exhibit diverse discotic liquid crystal behavior, and this has been shown to continue through the related hybrids [8]. Series of metal-free and copper derivatives have been characterized and all show columnar mesophases. A preliminary analysis of the thermal properties by polarizing optical microscopy of the lead hybrids was performed and initially indicated transitions at 63 ^{o}C and 70 ^{o}C for **8PbTBTAP** and **8PbTBMAP** respectively, with clearing to isotropic liquids occurring at ~240 ^{o}C for both samples. The transitions initially appeared reversible but with some hysteresis, producing textures that were ambiguous but consistent with formation of columnar hexagonal phases. For **8PbTBMAP**, a further transition was observed at 116 ^{o}C and a texture consistent with a columnar rectangular mesophase is produced. However, although analysis by DSC (Supporting Information) showed transitions at the same temperatures, the high temperature transitions are unusually broad (15-50 ^{o}C) and not representative of transitions for pure liquid crystalline materials. The assignments are therefore tentative and considered with caution. It is known that related lead

phthalocyanines are prone to demetallation in moderately harsh conditions [15] and the results obtained here indicated that decomposition occurs on heating.

Crystals suitable for X-ray diffraction were obtained by slow crystallization from dichloromethane-methanol mixtures, and the solid-state structures show significant contrast to the known, closely related structures for the symmetrical non-peripherally substituted lead octaoctyl phthalocyanine (**8PbPc**) [15] and copper tetrabenzotriazaporphyrin (**8CuTBTAP**) [8b]. The structures of these two known derivatives are illustrated in Figure 3. As expected, in **8PbPc** the lead ion lies out of the macrocycle plane. The macrocycle itself deviates from planarity and a saddle-shaped conformation is observed. A similar distorted conformation has been reported for the related, shorter chain **6PbPc** derivative [16]. In contrast copper is located within the macrocycle in **8CuTBTAP** and, overall, the macrocycle is essentially planar. Importantly, in both cases the macrocycles are significantly offset in the crystal packing, with negligible interactions between the metal of one macrocycle and its neighbors.

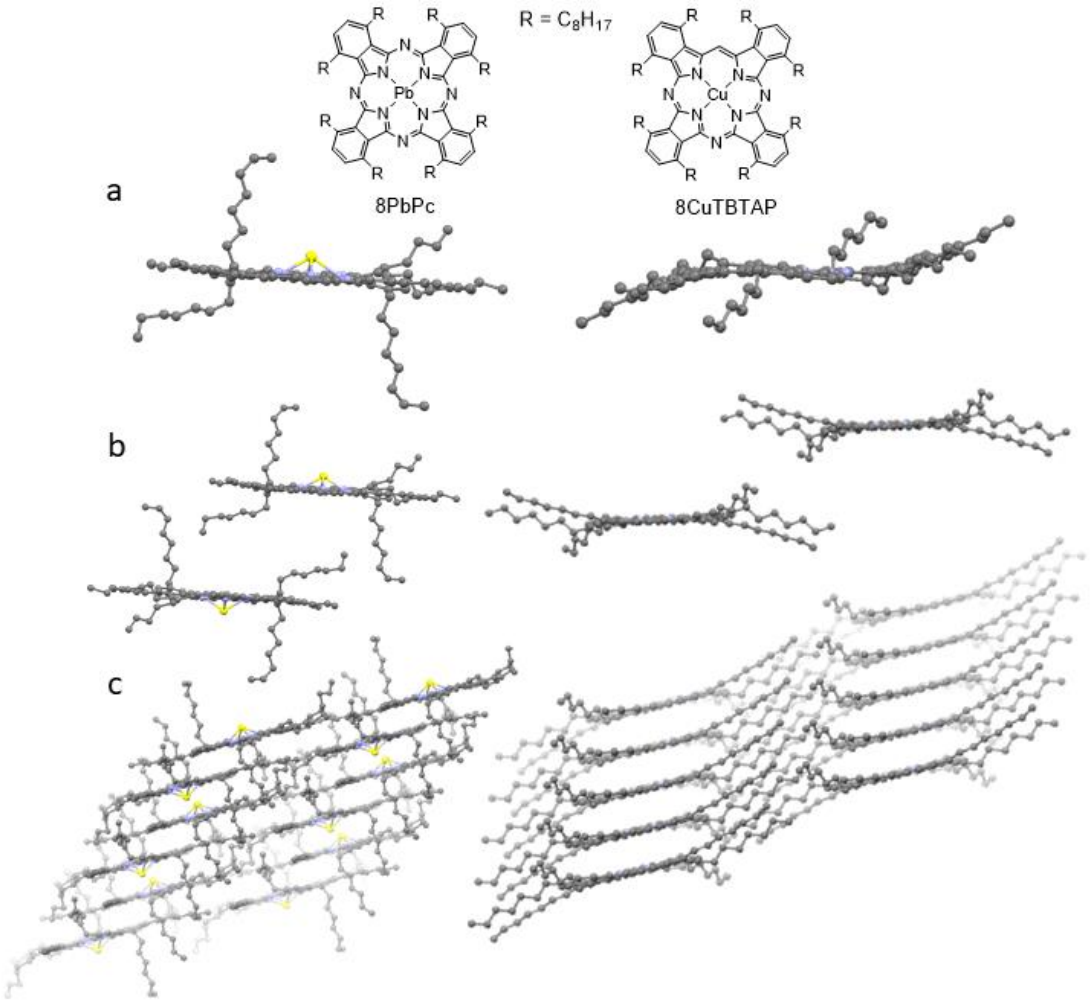

Figure 3. X-ray crystal structures of **8PbPc** [15] and **8CuTBTAP** [8b] showing (a) Side-on view of a single molecule; (b) unit cell packing; (c) extended packing structure showing offset stacks in tilted parallel columns.

The X-ray diffraction data for **8PbTBTAP** and **8PbTBMAP** indicate elements of disorder and possible modulation, making them challenging to solve. The structures were both solved in *P4cc* with inversion twinning, and it is immediately apparent that, despite the minimal molecular structural changes, the macrocycle arrangements are very different to the parent **8PbPc**. **8PbTBTAP** and **8PbTBMAP** are essentially isostructural. The molecular structures and packing arrangements are shown in Figure 4. Unusually and unlike other examples, the two new structures display stacks of face-to-face macrocycles in infinite columns in which the lead ions bridge between the central N4 units of the TBTAP/MAP macrocycles. In each case the Pb sits on a crystallographic 4-fold axis and appears possibly disordered with large Q-peaks above and below the atom. All attempts to model this disorder failed, so the Pb atoms were refined anharmonically, which accounts for the Q-peaks. Separation along the stacks is closer in **8PbTBMAP** compared to **8PbTBTAP**, with calculated average Pb-Pb distances 3.8794(2) Å and 3.9066(2) Å respectively. This observation is in line with the previously observed increase in central cavity size as nitrogen bridges are replaced by methines [8a].

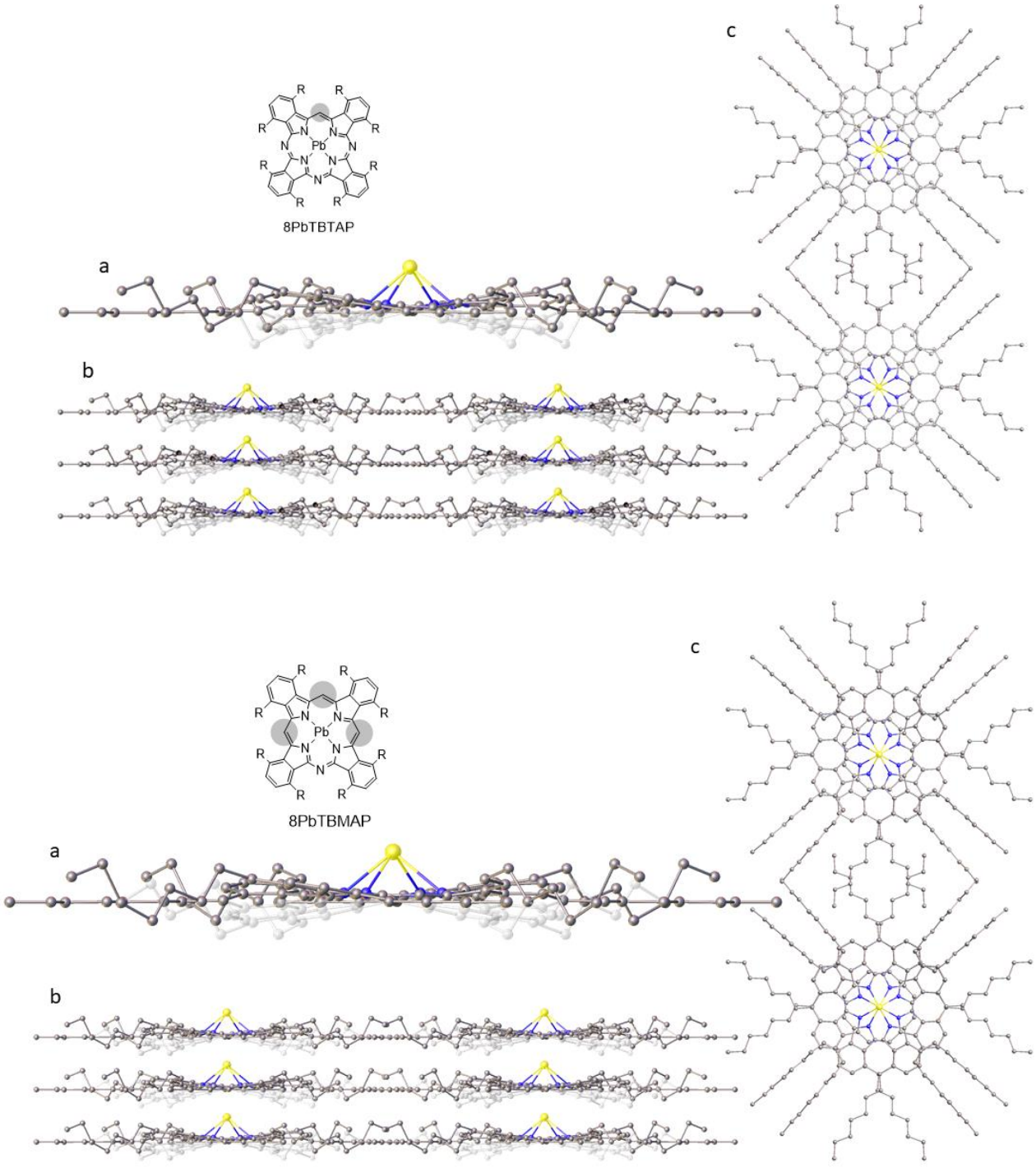

Figure 4. X-ray crystal structures of **8PbTBTAP** (top) and **8PbTBMAP** (bottom) showing (a) Side-on view of a single molecule; (b) unit cell packing (side) and (c) top showing face-to-face stacking of the macrocycles and bridging of lead ions through the infinite columnar stacks. Ghosted atoms and bonds indicate the disorder (a and b).

In conclusion, we report the synthesis of the full range of non-peripherally substituted lead phthalocyanine-tetrabenzoporphyrin hybrids. Lead insertion proceeds smoothly from the isolated metal-free hybrids and in the case of two derivatives (**8PbTBTAP** and **8PbTBMAP**) the final compounds were isolated as crystalline solids in sufficient quantity to

allow more in-depth characterization. The crystal structures of these two hybrids have been solved and are significantly distinct from the parent lead phthalocyanine (**8PbPc**). In the new hybrid structures the macrocycles form infinite co-facial stacks in which lead ions bridge between the N_4 planes.

Acknowledgements

We thank CONACYT, Mexico, and UEA for funding (LXS-V). MJC gratefully thanks the Leverhulme Foundation for the award of a Leverhulme Emeritus Fellowship. SJC and GJT thank the EPSRC for funding.

Supporting information

Crystallographic data have been deposited at the Cambridge Data Centre (CCDC) under deposition Nos. CCDC 2238769 [**8PbTBTAP**] and CCDC 2238770 [**8PbTBMAP**]. Copies can be obtained on request, free of charge, *via* www.ccdc.cam.ac.uk/conts/retrieving. html or from the Cambridge Crystallographic Data Centre, 12 Union Road, Cambridge CB2 1EZ, UK (fax:+44 1223-336-033 or email: deposit@ccdc.cam.ac.uk).

REFERENCES

1. a) Helberger JH, von Rebay A. *Liebigs Ann.* 1937, **531**, 279-287. b) Helberger JH, von Rebay A. *Liebigs Ann.* 1937, **531**, 205-218. c) Dent CE. *J. Chem. Soc*. 1938, 1-6; d) Barrett PA, Linstead RP, Tuey GAP, Robertson JM, *J. Chem. Soc*. 1939, 1809-1820; e) Barrett PA, Linstead RP, Rundall FG, Tuey GAP, *J. Chem. Soc.* 1940, 1079-1092.
2. a) Galanin NE, Kudrik EV, Shaposhnikov GP. *Russ. J. Gen. Chem.*, 2004, **74**, 282–285. b) Galanin NE, Yakubov LA, Kudrik EV, Shaposhnikov GP, *Russ. J. Gen. Chem.*, 2008, **78**, 1436–1440. c) Yakubov LA, Galanin NE, Shaposhnikov GP, *Russ. J. Org. Chem.*, 2008, **44**, 755–760. d) Galanin NE, Kudrik EV, Shaposhnikov GP, *Russ. J. Gen. Chem.*, 2005, **75**, 651–655. e) Galanin NE, Kudrik EV, Shaposhnikov GP, *Russ. J. Org. Chem.*, 2002, **38**, 1200–1203. f) Galanin NE, Shaposhnikov GP, *Russ. J. Gen. Chem.*, 2007, **77**, 1951–1954.
3. a) Leznoff CC, McKeown NB. *J. Org. Chem.*, 1990, **55**, 2186–2190. b) Tse Y-H, Goel A, Hu M, Lever ABP, Leznoff CC, *Can. J. Chem.* 1993, **71**, 742-753.
4. Makarova EA, Kopranenkov VN, Shevtsov VK, Lukyanets EA, *Chem. Heterocycl. Compd.* 1989, **25**, 1159-1164.
5. a) Khelivina OG, Berezin, BD, Petrov, OA, Glazunov AV, *Koord. Khim.* 1990, **16**, 1047-1052. b) Ivanova YB, Churakhina YI, Semeikin AS, Mamardashvili NZ, *Russ. J. Gen. Chem.*, 2009, **79**, 833–838. c) Cammidge AN, Cook MJ, Hughes DL, Nekelson F, Rahman M. *Chem. Commun.*, 2005, 930–932.
6. a) Cammidge AN, Chambrier I, Cook MJ, Sosa-Vargas L, in *Handbook of Porphyrin Science, Vol. 16* (Eds.: Kadish KM, Smith KM, Guilard R), World Scientific, New Jersey, London, 2012, pp. 331-404; b) Kalashnikov VV, Pushkarev VE, Tomilova LG. *Russ. Chem. Rev.* 2014, **83**, 657-675.
7. a) Kalashnikov VV, Pushkarev VE, Tomilova LG. *Mendeleev Commun.*, 2011, **21**, 92–93. b) Kalashnikov VV, Tomilova LG. *Macroheterocycles*, 2011, **4**, 209–210.
8. a) Cammidge AN, Chambrier I, Cook MJ, Hughes DL, Rahman M, Sosa-Vargas L. *Chem. – Eur. J.*, 2011, **17**, 3136–3146; b) Mack J, Sosa-Vargas L, Chambrier I, Hughes DL, Isare B, Poynter RJ, Powell AK, Cook MJ, Kobayashi N, *Inorg. Chem.* 2012, **51**, 12820-12833.

9. a) Díaz-Moscoso A, Tizzard GJ, Coles SJ, Cammidge AN. *Angew. Chem. Int. Ed.*, 2013, **52**, 10784–10787.b) Alharbi N, Díaz-Moscoso A, Tizzard GJ, Coles SJ, Cook MJ, Cammidge AN, *Tetrahedron*, 2014, **70**, 7370–7379. c) Alharbi N, Tizzard GJ, Coles SJ, Cook MJ, Cammidge AN. *Tetrahedron*, 2015, **71**, 7227–7232.
10. Tejerina L, Yamamoto S, López-Duarte I, Martínez-Díaz MV, Kimura M, Torres T. *Helv. Chim. Acta*, **103**, e2000085.
11. Alkorbi F, Díaz-Moscoso A, Gretton J, Chambrier I, Tizzard GJ, Coles SJ, Hughes DL, Cammidge AN. *Angew. Chem. Int. Ed.*, 2021, **60**, 7632-7636.
12. Sheldrick GM. *Acta Cryst.*, 2015, **A71**, 3-8.
13. Dolomanov OV, Bourhis LJ, Gildea RJ, Howard JAK, Puschmann H. *J. Appl. Cryst.*, 2009, **42**, 339-341.
14. Bourhis LJ, Dolomanov OV, Gildea RJ, Howard JAK, Puschmann H. *Acta Cryst. A*, 2015, **A71**, 59-71.
15. Sosa-Vargas LX, Chambrier I, MacDonald CJ, Coles SJ, Tizzard GJ, Cammidge AN, Cook MJ *J. Porphyrins Phthalocyanines* 2013, **17**, 511-521.
16. Burnham PM, Chambrier I, Hughes DL, Isare B, Poynter RJ, Powell AK, Cook MJ *J. Porphyrins Phthalocyanines* 206, **10**, 1202-1211.